# Nonlinear Mechanical Response of Amorphous Polymers Below and through Glass Transition Temperature

CATHERINE GAUTHIER, LAURENT DAVID, LAURENCE LADOUCE, RENAUD QUINSON, JO PEREZ

Laboratoire G.E.M.P.P.M.-u.a., CNRS 341-INSA, 69621 Villeurbanne, France

*Received 19 July 1996; accepted 29 October 1996*

**ABSTRACT:** The mechanical response of various amorphous polymers such as poly(methyl methacrylate), polycarbonate, polystyrene, and poly(ethylene terephthalate) were studied experimentally and theoretically. First, usual stress–strain constitutive equations were determined below and through their glass transition temperature. Further measurements were done to specify the double component of nonelastic strain (anelastic and viscoplastic). The analysis of all of the data was performed on the basis of a molecular theory of nonelastic deformation of amorphous polymers proposed by Perez et al. The main assumptions of this modeling are recalled in this article: the existence of quasi point defects corresponding to nanofluctuations of specific volume (concentration); the hierarchically constrained nature of molecular dynamics; and under the application of a stress, the nucleation and growth of shear microdomains (anelastic strain) until they ultimately merge irreversibly with one another (viscoplastic strain). Recently, developments based on the description of the dislocation dynamics were introduced. To account for strain hardening effect at large strains, the rubberlike elasticity formalism was included. The accuracy of the analysis in describing a high stress mechanical test was illustrated in a large range of temperatures. © 1997 John Wiley & Sons, Inc. J Appl Polym Sci **65:** 2517–2528, 1997

**Key words:** mechanical response; amorphous polymers; glass transition temperature

## INTRODUCTION

Many glassy polymers that exhibit attractive mechanical properties at room temperature have been extensively investigated and their constitutive equations have been determined in wide temperature and strain rate ranges. In the glassy state, amorphous polymers may exhibit plastic or brittle behavior under the action of large stresses. Here we deal solely with the former. It has been repeatedly noted in the literature that ductile behavior is easily observed in glassy polymers from the temperature of the glass transition ($T_g$) down to the temperature of the $\beta$ mechanical relaxation ($T_\beta$). This well-known empirical correlation illustrates the important role that molecular chain mobility plays in plastic deformation. Moreover, two temperature ranges are generally distinguished.[1,2] In the rubbery state, at $T > T_g$ the behavior of the polymer is explained in terms of rubber elasticity and chain reptation. Below $T_g$ the cohesion of an amorphous polymer in the glassy state is mostly due to intermolecular interactions. Within the intermediate temperature range, the glass transition and the main mechanical relaxation occurs and a combination of both phenomena has to be considered. As reviewed by Mangion et al.,[3] different physical approaches have been proposed to provide a description of the plastic behavior of glassy polymers.[4–8] Although it is generally well accepted that plastic deformation is a thermomechanically activated process, the nature of the related elementary motion is not always well defined. In the last few years at-

*Correspondence to:* Dr. C. Gauthier.

Journal of Applied Polymer Science, Vol. 65, 2517–2528 (1997)
 CCC 0021-8995/97/122517-12

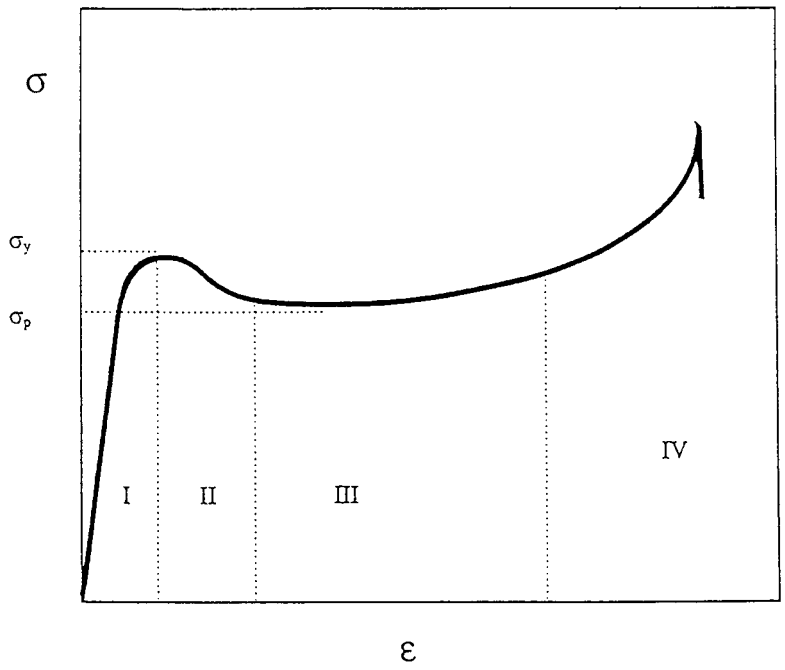


**Figure 1** Typical stress–strain curve for an amorphous polymer strained with a constant crosshead speed.

tempts were made in our group to relate the viscoelastic and viscoplastic deformations of amorphous materials to their microstructural state.[3,9–12] The following recalls the general physical concepts originally developed to interpret the behavior of amorphous polymers in both linear and nonlinear domains. Recent progress based on the description of the dislocation dynamics are introduced. In addition, the description is extended to the range of temperature above $T_g$ by including the contribution of rubberlike elasticity. Calculations involving different typical glassy polymers will be compared to experimental data obtained from high stress mechanical tests below and through the glass temperature.

## EXPERIMENTAL

### Typical Stress–Strain Behavior of Glassy Polymers Below $T_g$

The mechanical behavior of four quite typical glassy polymers—polycarbonate (PC), polystyrene (PS), poly(methyl methacrylate) (PMMA), and poly(ethylene terephthalate) (PET)—were investigated. As advised in standard textbooks, the compression or shear tests are best suited to study the sub-$T_g$ plastic deformation. Because parts of these experimental results were published elsewhere, we shall only review some of the most important results to highlight the deformation mechanisms. Experimental data are illustrated with only one of the polymers, but we qualitatively obtained the same for all the above-mentioned polymers.

Figure 1 shows the general features of the stress–strain curve of a glassy polymer strained using a constant crosshead speed. This curve exhibits four different typical parts. At first the curve consists of a nearly straight initial part corresponding to the elastic followed by the viscoelastic response of the polymer (for strain generally lower than 0.1). The initial slope of the curve is near the Hookean modulus but already corresponds to a partly relaxed response. The decrease of this slope coincides with the development of anelastic strain in the sample. In domain II (associated with the yield process) the stress reaches a maximum value often called yield stress, $\sigma_y$ and then decreases toward a minimum value $\sigma_p$ (plastic flow stress). Domain III corresponds to the region where the stress is minimum and almost independent of strain (stationary conditions). Then at high strain, the stress increases once again; the significant entropic stresses due to molecular orientation cause strain hardening. Finally, strain hardening appears to be gradually

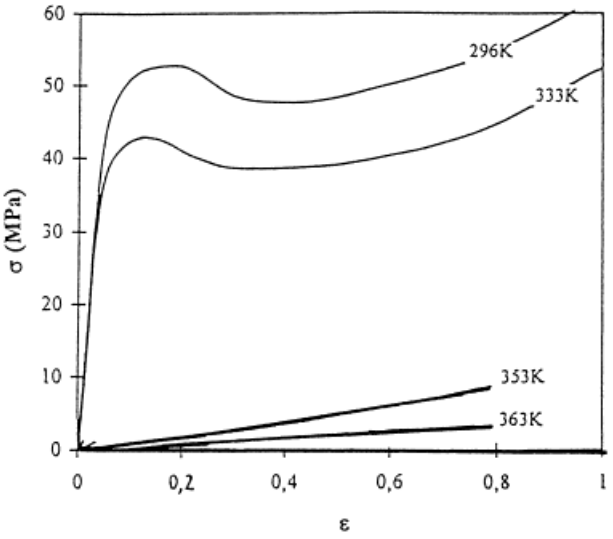


**Figure 2** Stress–strain curve for amorphous PET at various temperatures ranging between 296 and 363 K (plane strain test, $\dot{\varepsilon} = 8.3 \times 10^{-3}\ s^{-1}$, $L_0 = 0.875$ mm, $S_0 = 100\ mm^2$).

more important prior to breaking. It should be noted here that this figure corresponds to true stress–strain data and thus does not include plastic instabilities phenomena that will not be considered here. We add that the behavior law changed slightly with the type of mechanical test (compression, tensile, or shear).[13]

### Effect of Temperature on Mechanical Properties of Glassy Polymers

The curves displayed in Figure 2 illustrate the biaxial compression behavior of amorphous PET (aPET) for four typical temperatures from 296 to 358 K. It is clear that the glass temperature transition ($T_g$ = 349 K for PET) separates two distinct regimes. In the glassy state, at $T < T_g$ the material exhibits the typical behavior as discussed above: a sharp yield point followed by a steady-state plastic regime and a gradual strain hardening before a break. When the temperature of the test increases, the initial slope (relaxed modulus), the yield stress, and the amplitude of the peak decrease. When the temperature becomes higher than $T_g$, the yield peak vanishes and the stress increases monotonously with strain. The general features of the curve then correspond to rubberlike behavior. The progressive evolution from the plastic strain hardening to the rubberlike behavior through the glass transition temperature was noted by authors who proposed the simple interpretation that the large strain behavior below $T_g$ is mostly controlled by entropic force developed by the polymer chains when they become oriented.[14] Although the entropic origin of the work hardening in the glassy state is acceptable, it appears that the hardening at large strains is much higher for a glassy polymer than for the corresponding rubberlike elasticity.

### Aspects of Nonelastic Deformation of Homogeneous Polymers

Figure 3 presents the respective contributions of anelastic and viscoplastic strain during a compression test for a PMMA sample, as determined by Quinson et al.[11] This curve highlights the main role played by the anelastic component in the yielding process until a strain value of about 0.3. Then, anelastic strain tends toward a constant value ($\varepsilon_{anstat}$) while the viscoplastic strain becomes the main component of the deformation: it is the plastic state of deformation. Beyond yielding, a remaining strain after unloading still persists at zero load for some time, which recovers at an observable rate if enough time or temperature is allowed. This corresponds to anelasticity, which is accompanied by structural changes and creates a high level of internal energy in the sample. Two groups found[11,12] that the internal energy excess is only related to anelasticity and may be removed from the deformed sample by waiting times or by heating. Incidentally, plastic deformation, which cannot be recovered at ambient temperature, starts only from anelastic sites. At temperatures above $T_g$, due to the high increase of molecular mobility, the entropic forces (due to molecular orientation) become high enough to allow "plastic strain" recovery.[15]

## PHYSICAL MODEL FOR MECHANICAL RESPONSE OF GLASSY POLYMERS

To relate the macroscopic behavior (as measured during a mechanical test) to local molecular motions, a theory was first developed in our group in the case of very small stress.[10] The main relaxation process (often called $\alpha$ relaxation) was described in terms of hierarchically correlated collective molecular motions. It was stated that the so-called $\beta$ process corresponds to precursor motions responsible for the $\alpha$ relaxation process. The correlation parameter increases with the disorder described in terms of local defects: nanofluctu-

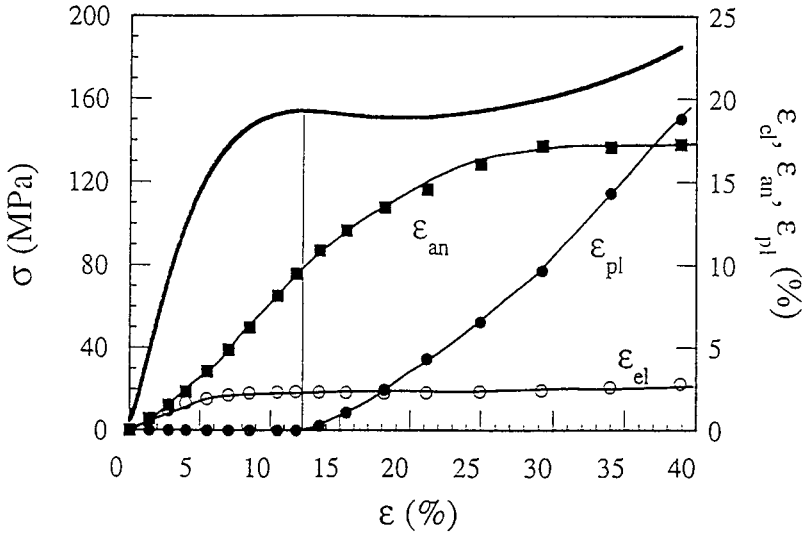


**Figure 3** Components of nonelastic deformation during stress–strain curve for amorphous PMMA ($T = 293$ K, $\dot{\varepsilon} = 2 \times 10^{-3}$ s$^{-1}$).

ations of density frozen in below the glass transition temperature, referred to as "quasi point defects" (QPDs). In our continuing effort toward the understanding of the molecular and microscopic bases of polymer mechanical properties, the modeling study was extended to large stress–strain.[3,16] The three main assumptions recalled above are specified herewith.

### Microstructural Aspect and Molecular Mobility

The polymer is considered as a packing of repeat units linked together through intra- and intermolecular forces. The concept of QPDs is introduced in the case of repeat units that exhibit with their first neighbors an increment of enthalpy, entropy, and consequently a nanofluctuation of density compared to a close packed arrangement of the same units. QPDs (concentration, $C_d$) correspond to positive or negative nanofluctuations of specific volume as well and determine the molecular mobility.

### Correlated Molecular Motions in Condensed Matter

The molecular dynamics that control the response to any field applied to an amorphous medium are supposed to be hierarchically constrained. Consequently, characteristic times of the anelastic process range between the time characterizing the elementary molecular motion (conformational change) assimilated to the $\beta$ relaxation time ($\tau_\beta$) and the time corresponding to the translational movement of a repeat unit over a distance equal to its size ($\tau_{\text{mol}}$). Previous analysis of the molecular mobility in amorphous polymers yields

$$\tau_{\text{mol}} = t_0\left(\frac{\tau_\beta}{t_0}\right)^{1/\chi} \tag{1}$$

where $t_0$ is a scaling parameter. The parameter $\chi (0 < \chi < 1)$ is a measure of the degree of hierarchical constraint molecular motions. It increases with $C_d$ between 0 (fully constrained situation) and 1 (constraint free situation). $\tau_\beta$ is well described by an Arrhenius law. At high stress ($>10^6$ Pa) the thermomechanical activation of the $\beta$ process yields

$$\tau_\beta(\sigma) = \tau_{0\beta}\exp\left[\frac{U_\beta\left(1 - \frac{\sigma}{\sigma_0}\right)^{3/2}}{kT}\right] \tag{2}$$

where $\sigma_0$ is the limit of the yield stress when the temperature becomes 0 K, the so-called Frenkel limit, and $U_\beta$ is the activation energy of the $\beta$ relaxation. Then $\tau_{\text{mol}}$ becomes $\tau_{\text{mol}}(\sigma)$.

$$\tau_{\text{mol}}(\sigma) = t_0\left(\frac{\tau_\beta(\sigma)}{t_0}\right)^{1/\chi} \tag{3}$$

### Nonelastic Deformation in Glassy State

The macroscopic deformation results from molecular motions that are polarized in the main shear

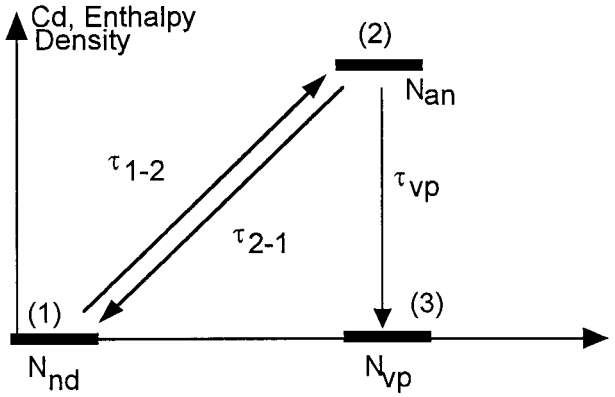


**Scheme 1** Description of the three different states occupied during the process of nucleation, growth, and coalescence of SMDs.

directions. These movements induce the nucleation and growth of shear microdomains (SMDs) limited by dislocation loops of Somigliana's type in some sites where molecular mobility is higher. SMDs are reversibly nucleated (anelastic strain) and the elastic stresses in the border of the SMDs (quite close to the stress field around dislocations in the crystals) can be restored when unloading. If the stress is applied for a long time or at high temperature, SMDs merge irreversibly with one another and that corresponds to viscoplastic strain that cannot be recovered below $T_g$ on a reasonable time scale.

### *Kinetic Aspect of Deformation Processes*

It can be derived from dislocation dynamics that the elastic energy associated with the dislocation loop that expands is opposite to the work of the stress related to the expansion. On this basis, a semiquantitative representation of the energy profile associated with the local region in which a SMD is nucleated and expands was discussed elsewhere.[16] In short, the whole energy profile falls with increasing applied stress. Consequently, increasing the stress results in nonlinear behavior corresponding to both an increase of the response amplitude and faster kinetics for occupying new states. Such a picture could explain the increase of the anelastic component of the response with stress because more numerous high energy sites are occupied and there is instantaneous strain recovery upon the release of mechanical stress.

To include the main results discussed above and in the literature,[11,12,15] the description of deformation processes is presented on Scheme 1. Three different states can be occupied during the process of nucleation, growth, and coalescence of SMDs. In short, applying a stress leads to the nucleation of SMDs that corresponds to the activation of sites from (1) to (2). This process is accompanied with a local increase of energy due to the disturbance of intermolecular van der Waals bonds. This stored energy corresponds on the one hand to the increase of disorder ($C_d$ increases) and on the other hand to the elastic energy associated with the dislocation loop. The system reaction to this nucleation process induces a drawback force related to the stored elastic energy. If unloaded the system returns to the equilibrium state by clearing the barrier from (2) to (1). With the constriction of SMDs, the microstructural state of the undeformed material is recovered (QPD concentration and consequently density and enthalpy). If the stress is high enough, the SMDs ultimately merge irreversibly with one another [barrier from (2) to (3)]. That implies the dissipation of the stored energy that corresponds to the local reorganization of intermolecular bounds: the polymer comes back to the microstructural characteristics of the nondeformed sample except for some local chain orientations.[12]

We can separate the total number of sites where such events would occur ($N_{\text{tot}}$) into two parts: low energy sites ($N_{\text{nd}} + N_{\text{vp}}$) and anelastic sites ($N_{\text{an}}$). Only the anelastic sites are the excited ones (higher energy state); that means that the viscoplastic sites that are in a low energy state are concerned with the SMD's nucleation. $N_{\text{tot}} = N_{\text{nd}} + N_{\text{an}} + N_{\text{vp}}$.

During a increment of time $dt$, we can express the variation of the number of excited sites:

$$\frac{dN_{\text{an}}}{dt} = \frac{N_{\text{tot}} - N_{\text{an}}}{\tau_{1-2}} - \frac{N_{\text{an}}}{\tau_{2-1}} - \frac{N_{\text{an}}}{\tau_{\text{vp}}} \qquad (4a)$$

Thus, three characteristic times are introduced to describe the dynamic of the system:

1. $\tau_{1-2}$ is the activation of anelastic strain [from well (1) to (2)],
2. $\tau_{\text{vp}}$ is the activation of plastic strain [from well (2) to (3)], and
3. $\tau_{2-1}$ is the recovery of anelastic strain [from well (2) to (1)].

Equation (4a) can also be written as

$$\frac{dN_{\text{an}}}{dt} = \frac{N_{\text{tot}}}{\tau_{1-2}} - \frac{N_{\text{an}}}{\tau_{\text{an}}} \quad \text{with}$$

$$\frac{1}{\tau_{\text{an}}} = \frac{1}{\tau_{1-2}} + \frac{1}{\tau_{2-1}} + \frac{1}{\tau_{\text{vp}}} \qquad (4b)$$

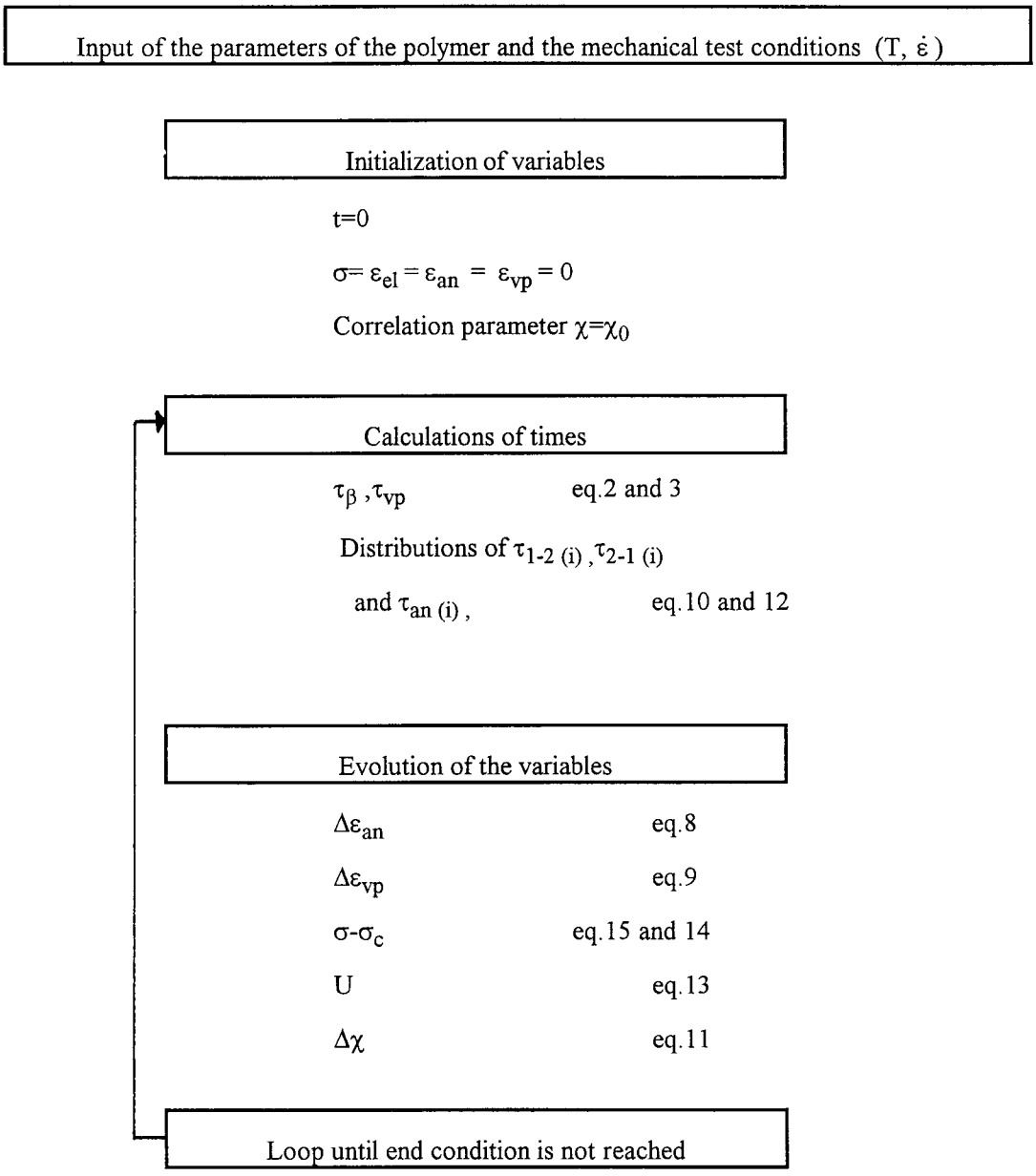


**Scheme 2** Algorithm of the program.

Moreover, the viscoplastic event occurs with a kinetic given by

$$\frac{dN_{vp}}{dt} = \frac{N_{an}}{\tau_{vp}} \tag{5}$$

A steady state of plastic deformation is reached when kinetics of anelastic and viscoplastic deformation are equal, meaning when nucleation of the SMD is equal to the coalescence. At this moment the values of the anelastic component and the QPD number are kept constant. In the steady state,

$$\frac{dN_{an}}{dt} = 0 \tag{6}$$

So, the number of anelastic sites in the steady state ($N_{anstat}$) is given by

$$N_{anstat} = \frac{\tau_{an}}{\tau_{1-2}} \cdot N_{tot} \tag{7}$$

And eq. (4b) becomes

**Table I Parameters for PMMA and PET**

| | PET | PMMA |
|---|---|---|
| $T_g$ (K) | 349 | 380 |
| $\tau_{0\beta}$ (s) | $3 \times 10^{-16}$ | $2.6 \times 10^{-16}$ |
| $U_\beta$ (kJ/mol) | 55 | 78 |
| $t_0$ (s) | $3 \times 10^{-12}$ | $4.5 \times 10^{-9}$ |
| $\chi$ ($T < T_g$) | 0.28 | 0.3 |
| $\chi$ ($T > T_g$) | $0.28 + 9 \times 10^{-3}\,(T - T_g)$ | $0.3 + 5.5 \times 10^{-3}\,(T - T_g)$ |
| $B_{\text{Gauss}}$ | 0.7 | 1.2 |
| $\sigma_0$ (Pa) | $4 \times 10^8$ | $4.3 \times 10^8$ |
| Gel (Pa) | $1.6 \times 10^9$ | $3 \times 10^9$ |
| $G_c$ (Pa) | $1.1 \times 10^6$ | $0.75 \times 10^6$ |
| $G_{\text{anstat}}$ (Pa) | $2.8 \times 10^8$ | $2 \times 10^8$ |
| $A_{\text{an}}$ | 0.6 | 1 |
| $A_{\text{vp}}$ | 0.1 | 0.015 |
| $A_u$ (kJ/mol) | 50 | 100 |

$$\frac{dN_{\text{an}}}{dt} = \frac{N_{\text{anstat}} - N_{\text{an}}}{\tau_{\text{an}}} \tag{4c}$$

Each event can be associated with an increment of strain. Thus, the dynamics of the system can be summarized by eqs. (8) and (9) for both components of nonelastic strain.

$$\frac{d\varepsilon_{\text{an}}(t)}{dt} = \frac{\varepsilon_{\text{anstat}} - \varepsilon_{\text{an}}(t)}{\tau_{\text{an}}} \tag{8}$$

$$\frac{d\varepsilon_{\text{vp}}(t)}{dt} = \frac{\varepsilon_{\text{an}}(t)}{\tau_{\text{vp}}} \tag{9}$$

The molecular motions responsible for the anelastic component of the strain are similar to those implied in the low temperature part of the $\alpha$ relaxation. That means that the jump of barrier (1) to (2) is obtained through correlated thermomechanically activated movements so that $\tau_{\text{an}}$ and $\tau_{\text{vp}}$ must be related to $\tau_{\text{mol}}(\sigma)$.

At this point it is necessary to realize that, because the environment of molecules forming the defects varies as a result of molecular disorder, the value of $\tau_{\text{an}}$ is not unique but is distributed between a low value corresponding to the activation of an elementary molecular motion ($\tau_\beta$) and a high value assimilated to $\tau_{\text{mol}}(\sigma)$. In practice, we chose to incorporate the disordered characteristic of the molecular structure in terms of a Gaussian distribution of the correlation parameter $\chi$. It is thus numerically possible to determine the time variations of anelastic and viscoplastic strain increments for each population with a correlation parameter $\chi_i$ between 1 and $\chi_m$.

$$\tau_{1-2} = \tau_{\text{mol}}(\sigma, \chi_i) \tag{10}$$

with $1 > \chi_i > \chi_m$. Moreover, during the deformation, two competing effects occur.

1. The first is an increase of $C_d$ from an equilibrium (stress free) value due to the propagation of dislocation lines (proportional to the anelastic component). This increase of $C_d$ or, in other words of the overall mobility, will in turn cause an increase of the value of the correlation exponent $\chi_m$.
2. The second effect is a decrease of the mobility when macromolecules become oriented (related in first approximation with viscoplastic strain), which corresponds to a decrease of $\chi_m$.

$$\chi_m = A_{\text{an}} \cdot \varepsilon_{\text{an}} - A_{\text{vp}} \cdot \varepsilon_{\text{vp}} \tag{11}$$

This last point will be discussed later.

The strain recovery of anelastic deformation is due to molecular motions similar to those responsible for MDC nucleation, but in an opposite way. The higher the stored energy, the faster is the recovery.[7–17] To describe this recovery effect, we step in the characteristic time $\tau_{2-1}$ the energy $U$ associated with the elastic energy of the dislocation loops. In a first approximation $U$ is a linear function of the anelastic component.

$$\tau_{2-1} = \tau_{\text{an}}(-\sigma)\exp\left(-\frac{U}{kT}\right) \tag{12}$$

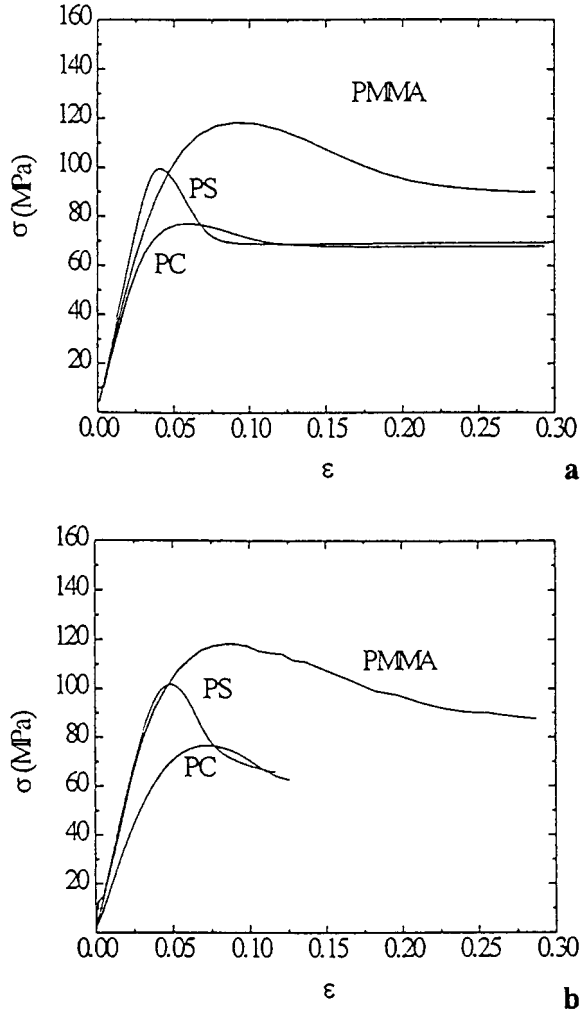


**Figure 4** (a) Calculated curves of PMMA, PS, and PC (compression test at $T = 293$ K, $\dot{\varepsilon} = 1.6 \times 10^{-3}\ s^{-1}$) and (b) experimental data.

$$U = A_u \cdot \varepsilon_{an} \tag{13}$$

At last the motions that are implied in plastic deformation are translational; they correspond to the high temperature part of the $\alpha$ relaxation. The characteristic time for the viscoplasticity is chosen equal to $\tau_{mol}(\sigma, \chi_m)$.

## Analysis of Rubbery Elasticity

To date, numerous models were proposed for the interpretation of rubberlike elasticity, the origin of which is mainly entropic. Basic relationships were established from statistical calculations that considered an ideal network constituted of freely jointed segments of chains.[2] Several important postulates were used in the development of the molecular theories of rubberlike elasticity. The first one specifies that although intermolecular interactions are certainly present in elastomers, they are independent of chain configuration. The assumption is that rubberlike elasticity is entirely of intramolecular origin. In the simplest approach an affine deformation is assumed: each chain of the network is deformed as the macroscopic specimen. Most theories assume additionally that the network chains have end to end distances obeying a Gaussian distribution. Considering the loading mode, this leads to an internal stress given by

$$\sigma_c = G_c(\lambda^2 - \lambda^{-1}) \quad \text{(tensile, uniaxial compression)}$$
$$\tau_c = G_c(\lambda - \lambda^{-1}) \quad \text{(shear)}$$
$$\sigma_c = G_c(\lambda - \lambda^{-3}) \quad \text{(biaxial compression)} \tag{14}$$

with $G_c = nkT$, where $n$ is the density of chain sections per unit volume, k is the Boltzmann constant, and T is the absolute temperature; and $\lambda = l/l_0$ is the change in sample dimension.

Some refinement can be introduced based on the concept of limited extendability for chain portions of finite length (the average number of freely jointed segments per chain being noted $N$). In recent years different topologies were proposed that differ by the organization of the chains in the representative network cell. In the classical model of Wang and Guth, a cubic cell with three chains per cell is considered.[18] Arruda and Boyce[19] suggested distributing eight chains per cell whereas

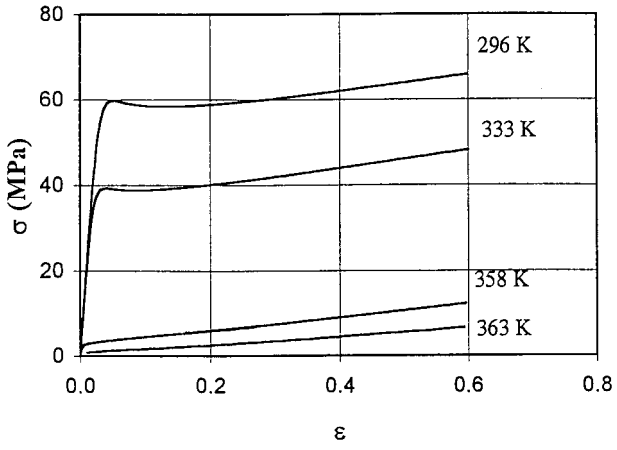


**Figure 5** Calculated curves of aPET at various temperatures ranging between 296 and 363 K (plane strain test, $\dot{\varepsilon} = 8.3 \times 10^{-3}\ s^{-1}$, $L_0 = 0.875$ mm, $S_0 = 100\ mm^2$).

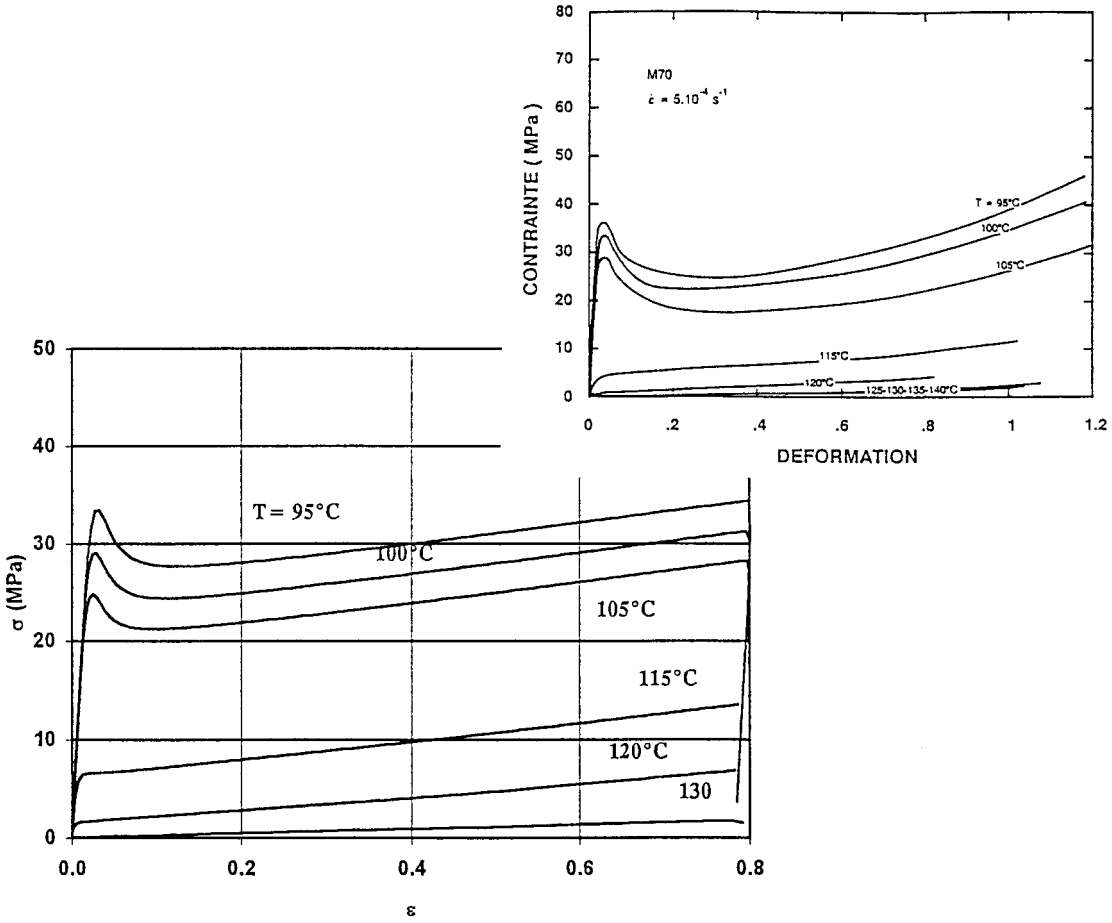


**Figure 6** Calculated curves of PMMA at various temperatures ranging between 368 and 403 K (compression test, $\dot{\varepsilon} = 2 \times 10^{-3}\ s^{-1}$).

Wu and Van der Gissen[20] proposed a network cell with a random number of chains. In the rubbery state whole calculations (even the simplest) are satisfactory to fit the stress–strain curves obtained by classical mechanical tests (tensile compression, shear, etc.) until strain is equal to 1. For higher elongation the simplest modeling gives a less impressive description. Nevertheless, results in the literature[14] indicate that the use of advanced modeling is complicated by the choice of $N$ that should be adjusted with temperature, the type of mechanical test (tensile, compression, etc.), or the strain rate. In particular, when applied to describe the strain hardening in the glassy state, these calculations lead to unexpected very low $N$ values. Thus, in this work eq. (14) was chosen to calculate the rubberlike elasticity behavior and experimental data were satisfactorily reproduced above $T_g$.

Below $T_g$ the recorded stress corresponds to the sum of two components: the component ($\sigma_c$) corresponding to the contribution of the rubberlike elasticity and the component relative to the activation of plasticity. The first component is described by way of eq. (14); the second one is obviously calculated by the physical analysis of nonelastic deformation developed in the preceding part. Because experimental data showed that the strain hardening increases when temperature of deformation decreases, the contribution of rubber elasticity to strain hardening, calculated from eq. (14), cannot be sufficient at lower temperature. But it appears that molecular mobility, which is related to the disorder, decreases when macromolecules become oriented. This probably happens when strain hardening occurs in the sample while macromolecules are stretched in the strain direction. That is why it seems reasonable to take into account the dependence of the correlation parameter $\chi$ on the amount of viscoplastic strain.

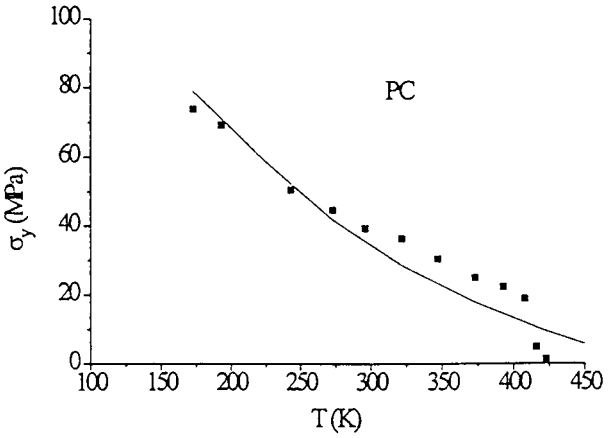


**Figure 7** The dependence of the yield stress versus temperature in the case of PC. (■) Calculations from the experimental data from Souahi.[21]

## DISCUSSION

In this part the modeling presented above will be applied to describe experimental data obtained in the usual mechanical tests. The calculations of creep and stress relaxation curves are beyond the scope of this article but can be simulated as well. When considering those mechanical tests that are performed using a constant crosshead speed for the nonelastic deformation, experimental considerations lead to[3]

$$d\sigma = R\left(V_0 - \left(\frac{d\varepsilon_{an}}{dt} + \frac{d\varepsilon_{vp}}{dt}\right)\cdot L_0\right)\cdot dt \quad (15)$$

where $V_0$ is the constant crosshead speed, $L_0$ and $S_0$ are the length and cross-sectional area of the sample, and $R_0$ is the rigidity of the testing machine. $R$ is given by

$$R = \frac{1}{\frac{S_0}{R_0} + \frac{L_0}{G}} \quad (16)$$

Incrementing the time by $\Delta t$ and using the values of $\Delta\varepsilon_{an}(t)$ and $\Delta\varepsilon_{vp}(t)$ given by eqs. (8) and (9), it is possible to calculate $d\sigma$. To introduce the rubberlike elasticity contribution, calculations are performed using an effective stress $\sigma_{act}$ given by

$$\sigma_{act} = \sigma - \sigma_c \quad (17)$$

A computer program was written to calculate the evolution of $\varepsilon$ and $\sigma$ versus time (see algorithm in Scheme 2). This program was designed to plot the $\varepsilon - \sigma$ graph. The parameters that need to be evaluated before running the program are listed in Table I for aPET and PMMA. Part of these parameters are evaluated from dynamic mechanical measurements: $G_u$, $G_c$, $\chi(T)$, $\tau_{0\beta}$, $U_\beta$, and $t_0$. At a very low temperature, yield stresses of order $0.1G$ ($G$, shear modulus) are reported for various thermoplastics, suggesting that yielding might occur at a stress close to the Frenkel theoretical shear strength. Three parameters remain that are adjusted once for the whole set of data. The first one ($A_{an}$) characterizes the linear relationship between $\chi$ and $\varepsilon_{an}$, the second ($A_{vp}$) that between $\chi$ and $\varepsilon_{vp}$, and the third ($A_U$) relies on $U$ and $\varepsilon_{an}$.

These relations were applied to calculate the constitutive equations of amorphous polymers below and through the glass transition temperature.

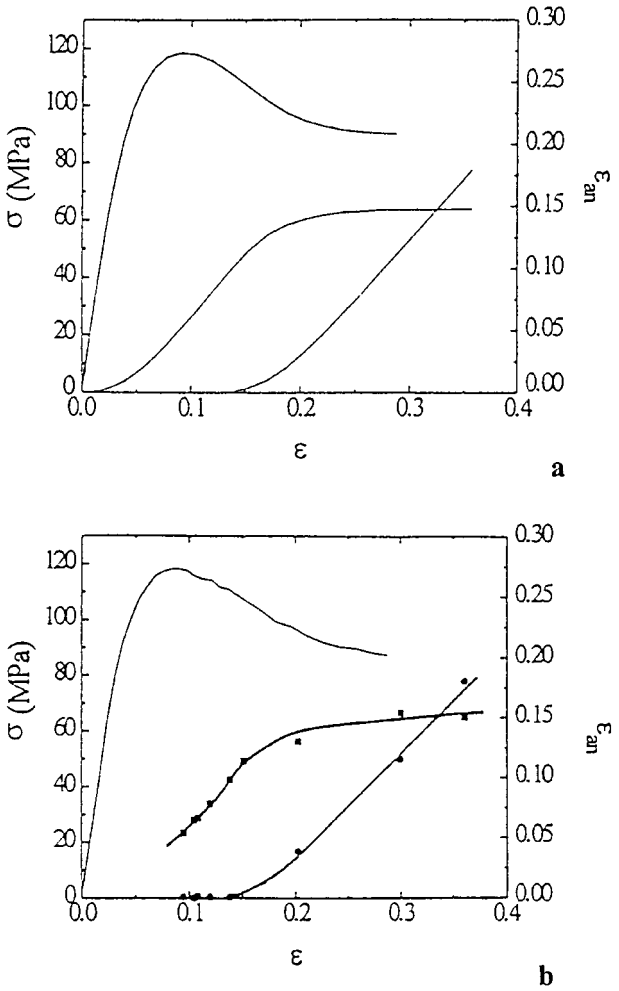


**Figure 8** Curves $\sigma$, $\varepsilon_{vp}$, and $\varepsilon_{an}$ versus $\varepsilon$ for PMMA (compression at 293 K and $2 \times 10^{-3}$ s$^{-1}$): (a) calculations and (b) experimental results.

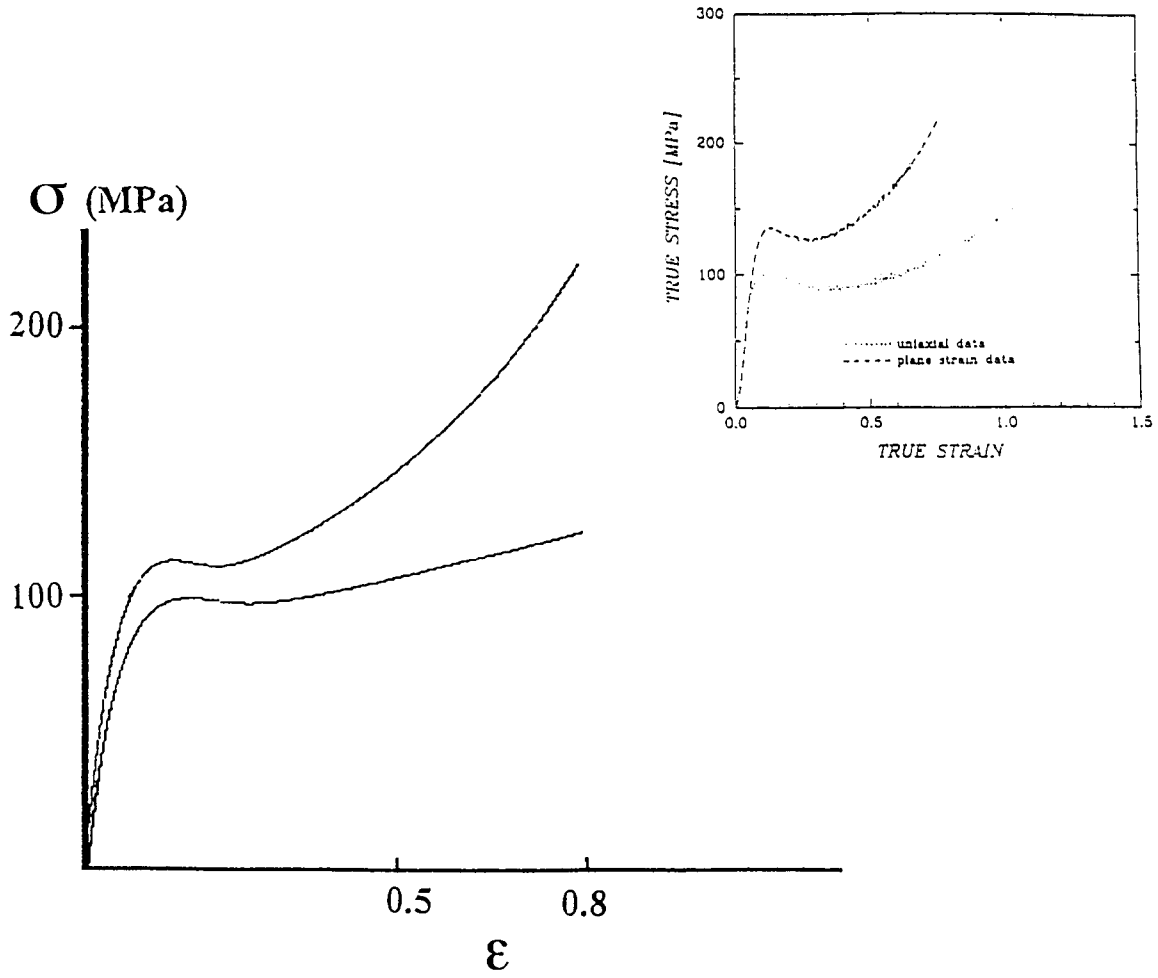


**Figure 9** Calculated curves of PMMA (compression test and plane strain test at room temperature, $\dot{\varepsilon} = 1 \times 10^{-3}\ s^{-1}$).

First we compared experimental data and calculated constitutive equations in the case of a compression test at 20°C and $\dot{\varepsilon} = 1.6 \times 10^{-3}\ s^{-1}$ for three different polymers: PC, PS, PMMA (Fig. 4). For each of these polymers, the shape of the curve, the value of $\sigma_y$ and $\sigma_p$, and the amplitude of the stress peak are reproduced well. A set of theoretical stress–strain curves for different temperatures is presented in Figure 5 for aPET ($\dot{\varepsilon} = 8.3 \times 10^{-3}\ s^{-1}$) and in Figure 6 for PMMA ($\dot{\varepsilon} = 5 \times 10^{-4}\ s^{-1}$). We can observe a good resemblance to the experimentally measured mechanical plastic response of aPET (Fig. 2) and PMMA (see Souahi[21]). The dependence of the yield stress versus temperature is illustrated in the case of PC (Fig. 7) and is compared to literature data.[22] Moreover, the model presented in this article further allows the independent determination of each contribution of the deformation (i.e., elastic, anelastic, and viscoplastic components) versus strain. The calculations clearly indicate that the anelastic strain gradually increases toward a plateau value while the viscoplastic one is negligible up to the time of appearance of the peak in stress (Fig. 8). We can add that the slight changes in the behavior law with the type of mechanical test (compression, tensile, shear) can also be reproduced (Fig. 9, compare with the results of Arruda et al.[13]).

The main points on which the accuracy of the analysis was improved can now be emphasized. From a general point of view, the description of the stress–strain curves of amorphous polymers were refined in

- the magnitude of the stress peak,
- the evolution of the yield stress with temperature and with strain rate, and
- the strain hardening phenomenon.

In addition, using the same set of parameters, the analysis can be applied in various types of mechanical tests: the usual mechanical tests performed using a constant crosshead speed, strain recovery upon the release of mechanical stress, and creep or stress relaxation tests.

## CONCLUSION

A model based on the concepts of QPDs, nucleation and expansion of SMDs, and hierarchically constrained molecular dynamics as originally proposed by Perez and coworkers [16] was applied to the description of the plastic behavior and the strain hardening of amorphous polymers. Experimental data obtained for the polymers PS, PMMA, PET, and PC were fit. The data described the various mechanical response of polymers when subjected to different modes of deformation using a unique set of parameter values for each polymer. The main interest of the approach is that the model not only reproduced experimental observations but also provided a general physical understanding of their features. Furthermore, we discussed the origin of the stress hardening observed at large strains in either the rubberlike state or the glassy state. At this point it appears that this physical description allows the interpretation of the behavior of amorphous polymers in linear and nonlinear domains using a unique set of parameters. The whole description of the usual stress–strain curves is now satisfactory from the development of anelasticity until the strain hardening process. The improvement of such an analysis is still going on in our group for a quantitative description of experimental data related to the thermostimulated recovery of strain after large anelastic and plastic strains.

## REFERENCES


1. I. M. Ward, *Mechanical Properties of Solid Polymers,* Wiley, New York, 1973.
2. J. E. Mark, in *Physical Properties of Polymers,* ACS Professional Reference Books, Washington, D.C., 1993, Chap. 1.
3. M. B. M. Mangion, J. Y. Cavaille, and J. Perez, *Phil. Mag. A.,* **66,** 773 (1992).
4. A. S. Argon, *Phil. Mag.,* **28,** 839 (1973).
5. P. B. Bowden and S. Raha, *Phil. Mag.,* **29,** 149 (1974).
6. B. Escaig, in *Plastic Deformation and Semi-Crystalline Materials,* B. Escaig and C. G'sell, Eds., Les Ulis: Les Éditions de Physique, Paris, 1985, p. 187.
7. O. A. Hasan and M. C. Boyce, *Polym. Eng. Sci.,* **35,** 331 (1995).
8. R. W. Rendell, K. L. Ngai, G. R. Fong, A. F. Yee, and R. J. Bankert, *Polym. Eng. Sci.,* **27,** 2 (1987).
9. J. Perez, *Physique et Mécanique des Polymères Amorphes,* Lavoisier Tec&Doc, Paris, 1992.
10. J. Y. Cavaille, J. Perez, and G. P. Johari, *Phys. Rev. B,* **39,** 2411 (1989).
11. R. Quinson, J. Perez, M. Rink, and A. Pavan, *J. Mater. Sci.,* to appear.
12. L. David, R. Quinson, and J. Perez, *Polym. Eng. Sci.,* submitted.
13. E. M. Arruda, M. C. Boyce, and H. Quintus–Bosz, *Int. J. Plast.,* **9,** 783 (1993).
14. C. G'sell and A. Souahi, in *Deformation Yield and Fracture of Polymers,* The Institute of Materials, London, 1994, p. 29/1.
15. E. F. Oleinik, O. B. Salamatina, S. N. Rudnev, and S. V. Shenogin, *Polym. Sci.,* **35,** 1819 (1993).
16. J. Perez, L. Ladouce, and R. Quinson, in *Deformation, Yield and Fracture of Polymers,* The Institute of Materials, London, 1994, p. 25/1.
17. G. W. Adams G. and R. J. Farris, *Polymer,* **30,** 1825 (1989).
18. M. C. Wang and E. J. Guth, *J. Chem. Phys.,* **20,** 1144 (1952).
19. E. M. Arruda and M. C. Boyce, *J. Mech. Phys. Solids,* **41,** 389 (1993).
20. P. D. Wu and E. Van der Giessen, *Mech. Res. Commun.,* **19,** 427 (1992).
21. A. Souahi, Ph.D. dissertation, INPL, Nancy, France, 1992.
22. C. G'Sell and A. J. Gopez, *J. Mater. Sci.,* **20,** 3462 (1985).